

hypothesis that the molecular structural linkage of integrin-cytoskeleton is an important pathway for the mechanotransduction<sup>(10)</sup>. Furthermore, when integrins were pulled by the RGD-coated micropipettes or microbeads, cell nuclei distorted and nucleoli redistributed along the direction of the applied force<sup>(11)</sup>. It has been known that nucleus deformation can be associated with cell deformation when cells are exposed to fluid shear stress<sup>(12)</sup>, compression<sup>(13)</sup>, stretching<sup>(14)</sup>, and flatten<sup>(15)</sup>, indicating direct mechanical linkages between cell surface receptors, cytoskeletons, and nuclei. To further address endothelial cell responses to mechanical forces, cell nucleus responses should be thus explored.

The objective of this study was to precisely quantify the effect of three different mechanical stimuli including fluid shear stress, cyclic stretching, and hydrostatic pressure on endothelial cell nucleus morphology. Mechanical contributions of cytoskeletal meshworks on nucleus morphology were also assessed after treatments with disruptive reagents.

**2. Materials and methods**

**2.1. Cell culture**

Bovine aortic endothelial cells were purchased from Cell Applications (San Diego, CA, USA). Endothelial cells were seeded into a tissue culture flask (Sumilon, Tokyo, Japan) with Dulbecco's modified Eagle medium (DMEM, Invitrogen, MD, USA) supplemented with 10% heat-inactivated fetal bovine serum (JRH Biosciences, KS, USA), penicillin and streptomycin (Invitrogen) and cultured at 37°C in a 5% CO<sub>2</sub>/ 20% O<sub>2</sub>/ 75% N<sub>2</sub> environment. Cells were confluent after 4-5 days and then passaged at a 1:4 split ratio in the flask using 0.05% trypsin-EDTA (Invitrogen). Before experiments, cells were seeded on a non-coated custom-built glass base culture dish with a diameter of 35 mm (Asahi Techno Glass, Tokyo, Japan) designed to allow shear stress- or hydrostatic pressure-imposed experiments. Cells were also seeded on a 0.1% gelatin-coated rectangular silicone membrane attached to the bottom of a silicone chamber for cyclic stretching-imposed experiments (see 2.2). Fully confluent cell populations from the 4th to 10th generation were studied.

**2.2. Application of three different mechanical stimuli**

The effect of three different mechanical stimuli, fluid shear stress, cyclic stretching and hydrostatic pressure, on nucleus morphology were studied with experimental methods previously reported<sup>(7),(8),(16)</sup>. Schematic diagrams of the experimental setup are shown in Fig. 1.

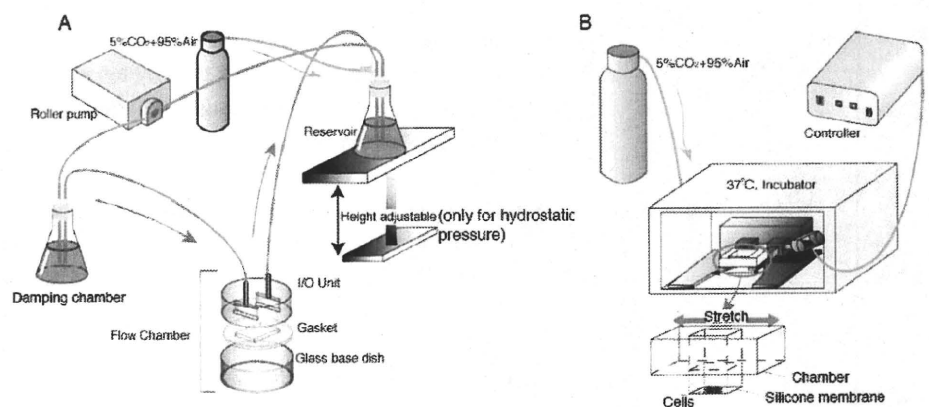


**Fig. 1** Schematic diagram of experimental setup for (A) fluid shear stress-imposed and hydrostatic pressure-imposed experiments and (B) cyclic stretching-imposed experiment.

For fluid shear stress-imposed experiments, the confluent cell monolayer was loaded into a parallel-plate flow chamber, as shown in Fig. 1A. In the flow chamber, an input/output (I/O) unit and a gasket were set in the glass-base dish to compose a flow field having a flow section of 0.5 mm in height and 14 mm in width. The channel flow can be approximated as two-dimensional fully developed laminar flow. Fluid shear stress of 2 Pa, which is comparable to the average value in aorta, was applied to cells for 24 h using a flow circuit consisting the flow chamber, two reservoirs, and a roller pump (Master Flex, IL, USA). During cell loading, the temperature of culture medium was maintained at 37°C by placing the damping chamber in a thermostatic chamber, and the pH controlled by pumping mixed gas (5% CO<sub>2</sub>/ 20% O<sub>2</sub>/ 75% N<sub>2</sub>).

For application of hydrostatic pressure, a similar assembly to that used for the fluid shear stress-imposed experiments was used. The height of the reservoir controls the hydrostatic pressure applied to the endothelial cell monolayer in the flow chamber. Using this system, hydrostatic pressures of 100 mmHg representing mean blood pressures in aorta was applied to the monolayer for 24 h. It should be noted that very slow fluid flow with shear stress of less than 0.1 Pa was applied to cells to perfuse nutrients and oxygen.

For cyclic stretching experiments, a silicone chamber (10 mm high x 25 mm wide x 44 mm long) with a cells-seeded silicone membrane having a square region of 20 mm x 20 mm was mounted on a commercially available cyclic stretcher consisting of a stepping motor and a controller (NS-600, Strex, Osaka, Japan), as shown in Fig. 1B. Prior to cell seeding, the silicone membrane was coated with 0.1% gelatin (Sigma, MO, USA). The silicone chamber was cyclically stretched up to a maximum strain of 10% at a frequency of 0.5 Hz for 6 h.

Each loading time were chosen to allow cells to undergo complete remodeling, referring to previous studies.

### 2.3. Disruption of cytoskeletal meshworks

In order to know how cytoskeletal meshworks can contribute to nucleus shape, actin filaments, intermediate filaments, and microtubules in unstimulated control cells were disrupted with treatment of 1 µg/ml cytochalasin D for 30 min at 37°C, 1 µM colchicines for 1 h at 37°C, and 5 mM acrylamide for 5 h at 37°C, respectively. Cell nuclei and cytoskeletons were fluorescently observed and morphological parameters of cell nuclei were analyzed (see 2.4 and 2.5).

### 2.4. Immunofluorescence staining

After mechanical tests, cells were incubated with 1 µg/ml CM-Dil (Molecular Probes, OR, USA) for 15 min at 4°C for staining cell membrane followed by an incubation with 0.4% SYTO13 (Molecular Probes), a marker of nucleic acids, for 20 min at 37°C for staining cell nuclei. Cells were also fixed with 10% formaldehyde in PBS (Dulbecco's phosphate-buffered saline without Ca<sup>2+</sup> or Mg<sup>2+</sup>, Wako, Osaka, Japan) for 5 min, permeabilized with 0.1% Triton X-100 in PBS for 5 min, and then incubated with 150 nM rhodamine-phalloidin (Molecular Probes) for 20 min at room temperature (RT) to study the effect of remodeling of actin meshwork on nucleus morphology.

For cytoskeleton disruption experiments, cells were incubated with 0.4% SYTO13 for 20 min at 37°C for staining cell nuclei before the disruption. After the disruption, cells were fixed with 10% formaldehyde in PBS for 5 min, permeabilized with 0.1% Triton X-100 in PBS for 5 min, and then incubated with 150 nM rhodamine-phalloidin for 20 min at RT, an anti-vimentin antibody (ProGen Biologics, MO, USA) for 20 min at RT followed by a Alexa Fluor 455-labelled anti-rabbit IgG antibody (Invitrogen) for 40 min at RT, and FITC-labelled anti- $\alpha$ -tubulin (Sigma) for 20 min at RT, for staining actin filaments, intermediate filaments, and microtubules, respectively. Nucleus shape and cytoskeletal

meshworks were fluorescently observed before and after the disruption.

Fluorescence images were captured using a confocal laser scanning microscope (FV1000, Olympus, Tokyo, Japan) with a 60x, NA 1.4 oil immersion objective (Uplan Apo, Olympus) as a series of X-Y optical slices at 0.35  $\mu\text{m}$  on Z axis.

### 2.5. Morphological Analysis

Morphological parameters of the nuclei including angle of orientation, Shape index<sup>(17)</sup>, projected area, and volume were evaluated using the public domain software (Image J 1.36b, National Institutes of Health, MD, USA). The cell outline was semi-automatically extracted producing cell area and perimeter. An equivalent ellipse for the cell outline, with an equal area and moment of inertia to the corresponding cell shape was then determined. The angle of orientation is defined as the deviation of the major axis of the equivalent ellipse from the direction of flow, by setting the cell orientation to a value ranging from 0° to  $\pm 90^\circ$ . For all images, the horizontal direction from left to right was defined as 0°. The angle of orientation was also evaluated for the cells. The shape index is defined as follows.

$$\text{Shape index} = 4\pi A / P^2 \quad (1)$$

where  $A$  is the cell area, and  $P$  the cell perimeter. The shape index is defined as 1.0 for a circle and approaches zero for highly elongated shape. Three-dimensional volume measurement of the nuclei was performed from the rendered images using a series of confocal slices.

### 2.6 Statistical Analysis

Statistical comparisons were made using unpaired Student's t-test and unpaired Welch's t-test for equal variance and unequal variance, respectively, unless otherwise stated. A value of  $p < 0.05$  was considered significant in all analyses. Statistical data were shown as mean + SD or mean  $\pm$  SD.

## 3. Results

### 3.1. Effects of mechanical stimuli on nucleus morphology

Fluorescence images of nucleus and cell membrane after the application of the three different mechanical stimuli were shown in Fig. 2. Changes in nucleus morphology were clearly observed in response to the mechanical stimuli, showing a close association with cell shape change. Actin meshwork for the three separate experiments was also shown in the figure. The actin cytoskeletons responded specifically to the three different mechanical stimuli. Statically cultured control cells exhibited a rounded shape, and thin, short actin filaments were centrally observed together with dense peripheral bands of actin filaments at the cell periphery. After exposure to fluid shear stress, cells exhibited elongation and orientation in the direction of flow with centrally located thick stress fibers parallel to the direction of flow, whereas, after exposure to cyclic stretching, cells elongated and oriented nearly perpendicular to the direction of stretch with thick stress fibers aligned with the major axis of cells. In contrast, cells exposed to hydrostatic pressure exhibited elongated shape with non-preferred orientation, with peripherally located long and thick filaments.

The angles of orientation of cells and their nuclei were shown in Fig. 3 for the three mechanical stimuli. For control cells, the angle of cell orientation was uniformly distributed between angles approaching  $-90^\circ$  or  $90^\circ$ . The similar tendency was observed for the angle of nucleus orientation. The percentages of sheared cells aligning between  $-30^\circ$  and  $+30^\circ$  were approximately 60% and 70% for the cells and their nuclei, respectively, indicating a close association of the cells with the nuclei in morphological change. Furthermore, the

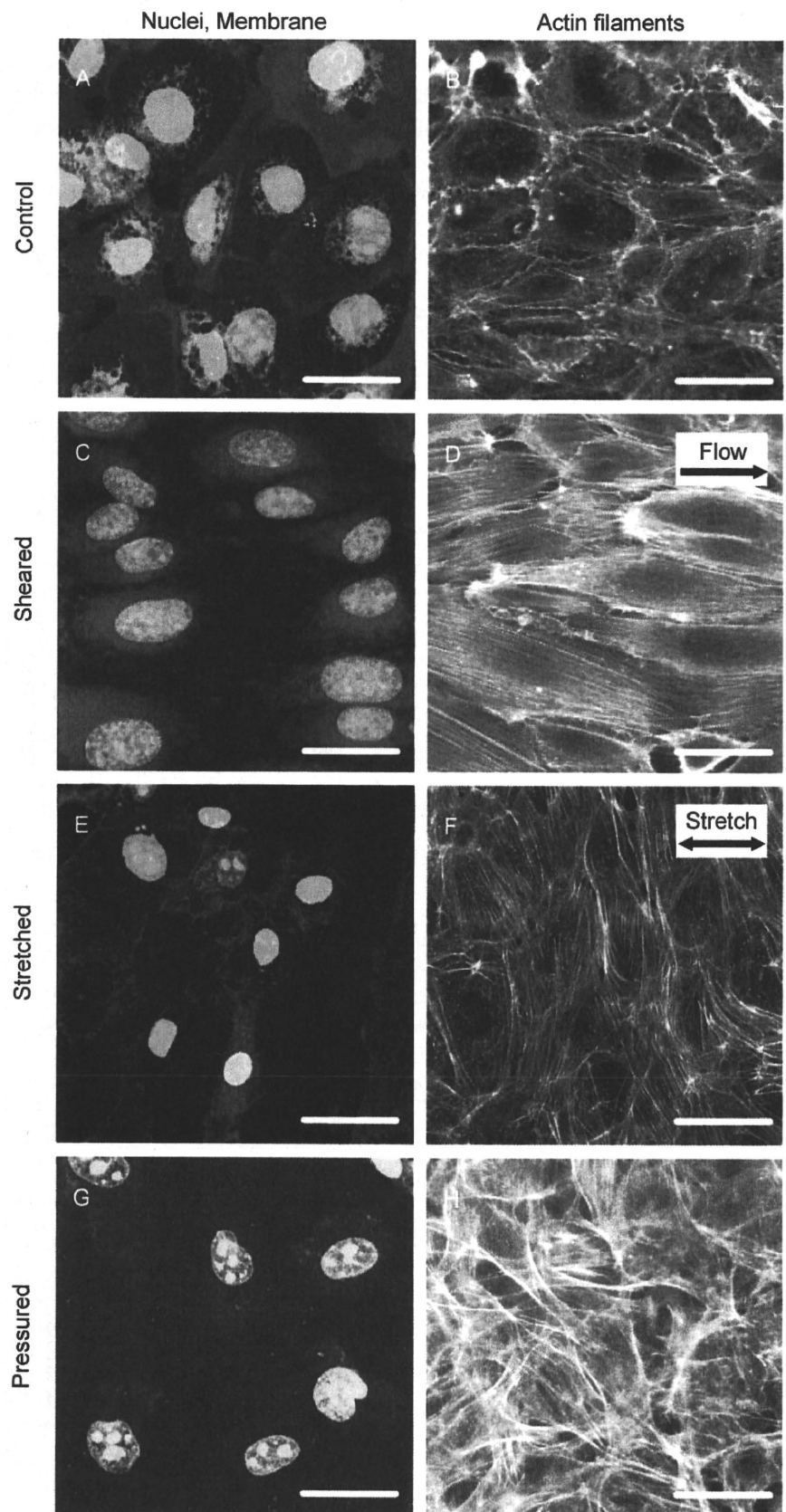


**Fig. 2** Fluorescence images of (A, C, E, G) cell nuclei and membrane and (B, D, F, H) actin filaments for statically cultured control, sheared, stretched, and pressured cells. Bars = 30  $\mu\text{m}$ .



percentages of stretched cells aligning between  $\pm 60^\circ$  and  $\pm 90^\circ$  were approximately 62% and 50% for the cells and their nuclei, respectively. In contrast, for pressured cells, the cells and their nuclei randomly aligned between  $-90^\circ$  and  $+90^\circ$  and no perceptible difference was found. However, there was a positive correlation between the cells and their nuclei in angle of orientation (Pearson's Product-Moment Correlation Coefficient  $r=0.633$ ,  $p < 0.001$ ).

Figure 4 shows the shape indices of the nuclei for the three mechanical stimuli. There were significant difference between both sheared ( $0.83 \pm 0.05$ ) and stretched cells ( $0.84 \pm$

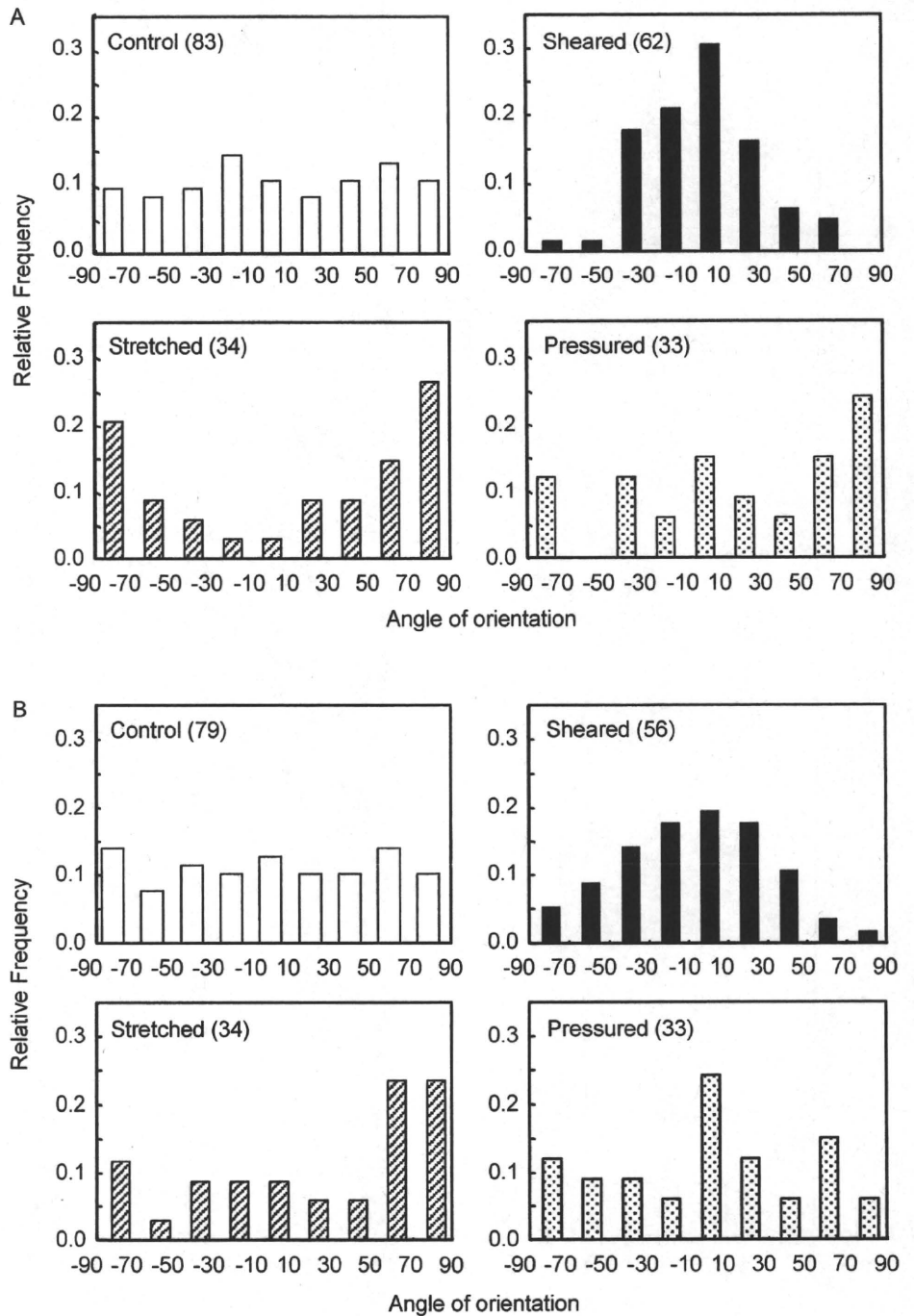


**Fig. 3** Change in the angle of orientation for (A) cells and (B) their nuclei after application of the three mechanical stimuli. The number in the parenthesis indicates the number of cells.

0.07) and control cells ( $0.87 \pm 0.04$ ,  $p < 0.01$  vs. sheared and stretched cells), whereas no significant difference between pressured cells ( $0.86 \pm 0.06$ ) and control cells.

The nucleus area and volume are shown in Figs. 5A and 5B, respectively for the three mechanical stimuli. In the area, compared to control cells ( $138 \pm 63$ ), a significant increase was found only in pressured cells ( $177 \pm 57$ ). No significant differences were found under the other two conditions ( $125 \pm 34$  and  $139 \pm 57$  for sheared and stretched cells, respectively). After exposure to mechanical stimuli, compared to control cells ( $825 \pm 295$ ),

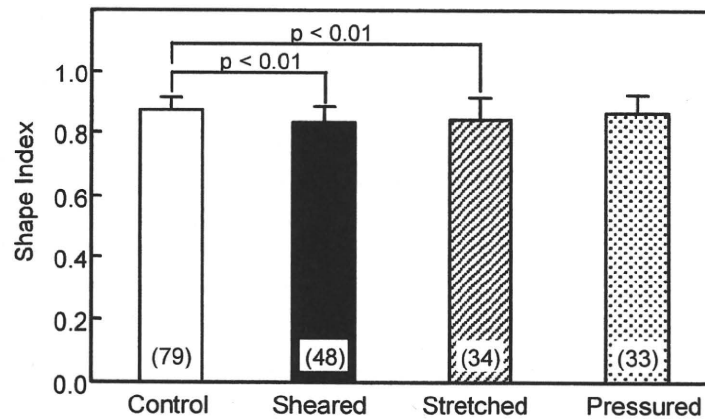


**Fig. 4** Change in the shape index of nuclei after application of the three mechanical stimuli. The number in the parenthesis indicates the number of cells.

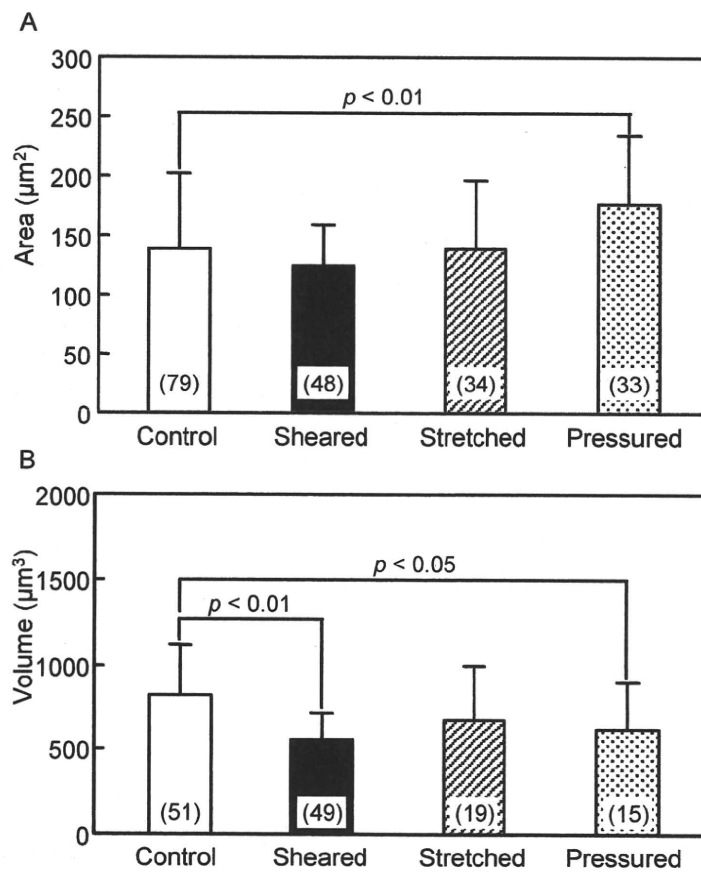


**Fig. 5** Changes in (A) area and (B) volume of nuclei after application of the three mechanical stimuli. The number in the parenthesis indicates the number of cells.

the nucleus volume significantly decreased for sheared cells ( $553 \pm 162$ ,  $p < 0.01$ ) and pressured cells ( $620 \pm 284$ ,  $p < 0.05$ ), whereas the volume decreased on average but there was no significant for stretched cells ( $676 \pm 322$ ). Taken together, these results indicate that the morphological change of the nuclei is not in an isotropic manner, and not likely due to passive deformation caused by the change in their surrounding mechanical environment such as development of stress fibers, but rather due to the active remodeling in response to mechanical stimuli, because cell nuclei can be assumed to be incompressible.

**3.2. Effects of cytoskeletal disruptions on nucleus morphology**

It was confirmed from fluorescence studies that actin filaments, intermediate filaments, and microtubules were well disrupted after treatment with the disruptive reagents. Changes in morphological parameters including the shape index, area, and volume of the nuclei after the disruption are shown in Fig. 6. The shape index showed no significant differences under the three conditions. Significant decreases were found in area under the three conditions ( $p < 0.05$ ). No significant difference was found in volume for disruption of actin filaments, whereas a significant increase was found for disruption of intermediate filaments ( $p < 0.05$ ). Disruption of microtubules induced a significant decrease in volume ( $p < 0.05$ ).

**4. Discussion**

The findings of this study indicate that the nuclei change their shape in accordance with different types of mechanical stimuli including fluid shear stress, cyclic stretching, and hydrostatic pressure, in a similar manner to that of the cells. Flaherty et al. <sup>(18)</sup> reported that endothelial cell nuclei showed differences in morphology at different locations around the circulatory system in canine. In regions of stronger hemodynamic forces, such as large arteries, the nuclei were elliptical in shape with their major axes being aligned with the direction of flow, whereas, in regions of weaker hemodynamic forces, the nuclei were more rounded and had no preferential direction. Flaherty et al. <sup>(18)</sup> also surgically changed the direction of flow exposed to the nuclei and found that the nuclei reoriented themselves in order to remain aligned with the flow. In this study, in vitro experiments here demonstrated that fluid shear stress may induce nucleus elongation and orientation in the direction of flow, which is in good agreement with the previous in vivo experiment.

Unlike fluid shear stress and hydrostatic pressure, cyclic stretching is defined as a strain-controlled mechanical loading. Therefore, it is important to pay particular attention to the terms, “passive deformation” and “(active deformation-induced) remodeling”. In

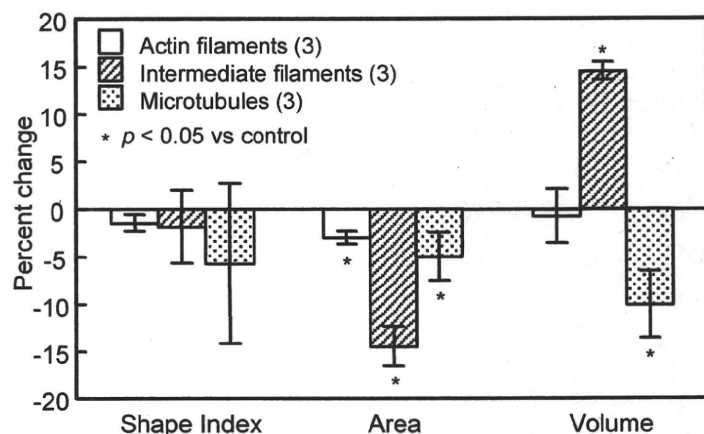


**Fig. 6** Changes in the shape index, area, and volume of nuclei after disruption of the three cytoskeletons. The number in the parenthesis indicates the number of cells.

general, observing the “passive deformation” of cells and cellular components including nuclei may take seconds or minutes after application of mechanical stimuli. If the nuclei passively deform, they would experience elongation in the direction of stretch by cyclic stretching. It has been reported that the nucleus is 9 times stiffer than the rest of the cell <sup>(11)</sup>. Taken together, it seems difficult for the nuclei to exhibit passive deformation even when being stretched up to 10%. Caille et al. <sup>(14),(19)</sup> reported that cell nuclei deformed less than the cytoplasm, which can be explained by the fact that the nuclei is much stiffer than the cytoplasm. In contrast, the “remodeling” may take hours to be observed. If the nuclei do not remodel and have enough stiff to resist the externally applied mechanical forces, no change in shape would be observed. However, the nuclei clearly showed alignment perpendicular to the direction of stretch at 6 hours after exposure to cyclic stretching, similar to that of their cells. Wang et al. <sup>(6)</sup> subjected bovine endothelial cells to 10% stretching at 0.5 Hz for 3 h and found that the cells reoriented specifically towards the direction of minimal substrate deformation. Furthermore, it is interesting to note that a numerical simulation showed that endothelial cells may respond to the applied flow in such a way as to minimize the total force on their nuclei <sup>(20)</sup>. Likewise, it is possible that cell nuclei remodel so as to minimize strain energy experienced by themselves.

After application of hydrostatic pressure, the nuclei neither showed, for the first time, any preferential alignment nor elongation. In our previous study, it was reported that bovine endothelial cells showed elongation with random cell orientation under pressured conditions, resulted in a significant decrease in the shape index <sup>(8)</sup>. This is probably because hydrostatic pressure is not a unidirectional stimulation unlike fluid shear stress and cyclic stretching. Little is still known of how mechanical forces are transmitted to local mechanosensing sites including focal adhesions <sup>(21)</sup> and intercellular junctions <sup>(22)</sup> where mechanical forces would be converted into biochemical signals, and to the nucleus <sup>(11)</sup> where mechanical forces would be possibly transduced into specific genetically regulated responses. In particular, it has been shown that external forces are transmitted by direct mechanical connections between surface receptors including integrins, cytoskeletal filaments and nucleoplasm <sup>(11)</sup>. Furthermore, finite element analysis was performed to explore the mechanotransduction pathway mediated by adhesion sites, cytoskeletons, and nuclei <sup>(23)</sup>. These studies may imply that alignment of cytoskeletal meshworks should be prerequisite for the remodeling of the nuclei. Pressured cells showed peripherally developed thick actin bundles. Therefore, it is hypothesized that pressured cells may have less unidirectional mechanical coupling between the nucleus and the cell surface where external forces are applied, towards the specific directions.

For hydrostatic pressure-imposed experiments, shear stress of less than 0.1 Pa was applied to cells to perfuse nutrients and oxygen. In our previous study <sup>(8)</sup>, it has been confirmed that there is no significant difference in cell morphology between cells exposed to shear stress of less than 0.1 Pa and control cells cultured statically in an incubator. Dewey et al. <sup>(24)</sup> reported that shear stress of less than 0.5 Pa did not induce any morphological change of bovine aortic endothelial cells. In contrast, Warabi et al. <sup>(25)</sup> reported that human umbilical vein endothelial cells cultured on a collagen-coated filter formed the line after exposure to low shear stress of 0.02 Pa in association with changes in gene expression. The difference in the critical shear stress may be due to the difference in the experimental conditions such as types of cells and extracellular matrices.

How cell nuclei remodel in response to mechanical stimuli is unclear. One possible idea to explain the mechanism of the nucleus remodeling would include the fact that there exists the nuclear lamina which is a fibrillar meshwork composed of intermediate filaments that lines the inner surface of the nuclear envelope. Galbraith et al. <sup>(26)</sup> applied fluid shear stress of ca. 1.5 Pa for 24 and showed that intermediate filaments aligned with the direction of fluid flow. Therefore, it is likewise possible for the cell nuclei to actively change their shape



possibly due to the reorganization of the nuclear lamina in response to mechanical stimuli.

It was also found in this study that three cytoskeletal meshworks including actin filaments, intermediate filaments, and microtubules could affect morphology of the nuclei even in statically cultured cells, indicating nucleus elastic recovery probably due to the release of mechanical constraints induced by cytoskeletal structures being the possible determinants in the deformation. However, the induced-deformation demonstrated different characteristics depending on the three types of the loss for cytoskeletons. It has been suggested that endothelial nuclei possibly have a mechanical contribution to intracellular force balances as a compression-bearing organelle, by demonstrating that the height of nuclei in cells is 0.59 of that of isolated nuclei under statically cultured conditions<sup>(12)</sup>. This implies that there exists pre-existing strain inside of the nuclei probably due to vertical compression caused by cytoskeletal meshworks. In this study, actin filaments had less contribution to the change in nucleus morphology compared to those by the other two cytoskeletons. This can be explained by the fact that well-developed actin meshwork is less distributed in the central portion of the cell, rather more at the cell periphery called dense peripheral bands. Manitois et al.<sup>(11)</sup> indicated that actin filaments potentially mediated force transfer to the nucleus at low strain and intermediate filaments effectively mediated force transfer to the nucleus. These filaments, therefore, work as molecular tensile elements as proposed separately<sup>(27)</sup>. In contrast, they also indicated that microtubules acted to hold intermediate filament lattice open and to stabilize the nucleus against lateral compression. In this study, intermediate filaments and microtubules were found to include a different mechanical role, indicating that intermediate filaments compressed the nucleus and microtubules did not. One may wonder whether microtubules can produce strong enough forces to stretch the nucleus. One possible idea to explain this include that disruption of microtubules means the loss of a compressive element from the viewpoint of intracellular force balance, leading to further compression induced by both actin filaments and intermediate filaments, and/or disruption of microtubules not only means the loss but also may affect intermediate meshwork by means of mechanical connections suggested in the previous study<sup>(11)</sup>. This is thus still unclear, but further studies should include an observation of subsequent events induced in intermediate filaments after disruption of microtubules.

In summary, this study addressed how three different mechanical stimuli including fluid shear stress, cyclic stretching, and hydrostatic pressure affect nucleus morphology. Fluorescence images showed that fluid shear stress and cyclic stretching induced cell elongation and orientation very specifically to the directions of flow and stretch, respectively, whereas hydrostatic pressure induced cell elongation at non-preferred orientation. Quantitative analysis on morphological parameters showed that cell nuclei also deformed in a similar fashion to the remodeling of cells, possibly indicating the direct mechanical linkages between cell surface receptors, cytoskeletal meshworks, and nuclei. Mechanical contributions of cytoskeletons to nucleus morphology were also assessed, showing the importance of the fact that cytoskeletal meshworks may contribute to pre-existing strain of the nuclei. It can be concluded that cell nuclei can sense external forces and remodel themselves as if they were structurally optimized.

### **Acknowledgements**

This study was supported by the Global Nano-Biomedical Engineering Education and Research Network Centre (Tohoku University Global COE Program) and Grant-in-aid for Scientific Research from the Ministry of Education, Culture, Sports, Science and Technology of Japan (No. 17200030).

### References

- (1) Levesque, M.J. and Nerem, R.M., The Elongation and Orientation of Cultured Endothelial Cells in Response to Shear Stress, *Trans ASME Journal of Biomechanical Engineering*, Vol. 107 (1985), pp. 341-347.
- (2) Nerem, R.M. Levesque, M.J., Cornhill, J.F., Vascular Endothelial Morphology As an Indicator of the Pattern of Blood Flow, *Trans ASME Journal of Biomechanical Engineering*, Vol. 103 (1981), pp. 172-176.
- (3) Kataoka, N. Ujita, S., Sato, M., Effect of Flow Direction on the Morphological Responses of Cultured Bovine Aortic Endothelial Cells, *Medical & Biological Engineering & Computing*, Vol. 36 (1998), pp. 122-128.
- (4) Ohashi, T., Sugawara, H., Matsumoto, T., Sato, M., Surface Topography Measurement and Intracellular Stress Analysis of Cultured Endothelial Cells Exposed to Fluid Shear Stress, *JSME International Journal Series C*, Vol. 43 (2000), pp. 780-786.
- (5) Davies, P.F., Flow-Mediated Endothelial Mechanotransduction. *Physiological Review*, Vol. 75, (1995), pp. 519-560.
- (6) Wang, J.H.-C., Goldschmidt-Clermont, P., Wille, J., Yin, F.C.-P., Specificity of Endothelial Cell Orientation in Response to Cyclic Mechanical Stretching, *Journal of Biomechanics*, Vol. 34 (2001), pp. 1563-1572.
- (7) Ohashi, T., Masuda, M., Matsumoto, T., Sato, M., Nonuniform Strain of Substrate Induces Local Development of Stress Fibers in Endothelial Cells Under Uniaxial Cyclic Stretching, *Clinical Hemorheology and Microcirculation*, Vol. 37 (2007a), pp. 37-46.
- (8) Ohashi, T., Sugaya, Y., Sakamoto, N., Sato, M., Hydrostatic Pressure Influences Morphology and Expression of VE-Cadherin of Vascular Endothelial Cells, *Journal of Biomechanics*, Vol. 40, No. 11 (2007b), pp. 2399-2405.
- (9) Sugaya, Y., Sakamoto, N., Ohashi, T., Sato, M., Elongation and Random Orientation of Bovine Endothelial Cells in Response to Hydrostatic Pressure: Comparison with Responses to Shear Stress, *JSME International Journal Series C*, Vol. 46, No. 4 (2003), pp. 1248-1255.
- (10) Chen, J., Fabry, B., Schiffrin, E.L., Wang, N., Twisting Integrin Receptors Increases Endothelin-1 Gene Expression in Endothelial Cells, *American Journal of Physiology Cell Physiology*, Vol. 280 (2001), C1475-C1484.
- (11) Maniotis, A.J., Chen, C.S., Ingber, D.E., Demonstration of Mechanical Connections Between Integrins, Cytoskeletal Filaments, and Nucleoplasm That Stabilize Nuclear Structure, *Proceedings of the National Academy of Sciences of the United States of America*, Vol. 94 (1997), pp. 849-854.
- (12) Deguchi, S., Maeda, K., Ohashi, T., Sato, M., Flow-Induced Hardening of Endothelial Nucleus As an Intracellular Stress-Bearing Organelle, *Journal of Biomechanics*, Vol. 38 (2005), pp. 1751-1759.
- (13) Guilak, F., Compression-Induced Changes in the Shape and Volume of the Chondrocyte nucleus, *Journal of Biomechanics*, Vol. 28 (1995), pp. 1529-1541.
- (14) Caille, N., Tardy, Y., Meister, J.-J., Assessment of Strain Field in Endothelial Cells Subjected to Uniaxial Deformation of Their Substrate, *Annals of Biomedical Engineering*, Vol. 26 (1998), pp. 409-416.
- (15) Ingber, D.E., Fibronectin Controls Capillary Endothelial Cell Growth by Modulating Cell Shape, *Proceedings of the National Academy of Sciences of the United States of America*, Vol. 87 (1990), pp. 3579-3583.
- (16) Ohashi, T. Ishii, Y., Ishikawa, Y., Matsumoto, T., Sato, M., Experimental and Numerical Analyses of Local Mechanical Properties Measured by Atomic Force Microscopy for Sheared Endothelial Cells, *Bio-Medical Materials and Engineering*, Vol. 12, No. 3 (2002), pp. 319-327.

- (17) Cornhill, J.F., Levesque, M.J., Herderick, E.E., Nerem, R.M., Kilman, J.W., Vasco, J.S., Quantitative Study of the Rabbit Aortic Endothelium Using Vascular Casts, *Atherosclerosis*, Vol. 35 (1980), pp. 321-337.
- (18) Flaherty, J.T., Pierce, J.E., Ferrans, V.J., Patel, D.J., Tucker, W.K., Fry, D.L., Endothelial Nuclear Patterns in the Canine Arterial Tree with Particular Reference to Hemodynamic Events, *Circulation Research*, Vol. 30 (1972), pp. 23-33.
- (19) Caille, N., Thoumine, O., Tardy, Y., Meister, J.-J., Contribution of the Nucleus to the Mechanical Properties of Endothelial Cells, *Journal of Biomechanics*, Vol. 35 (2002), pp. 177-187.
- (20) Hazel, A.L. and Pedley, T.J., Vascular Endothelial Cells Minimize the Total Force on Their Nuclei, *Biophysical Journal*, Vol. 78 (2000), pp. 47-54.
- (21) Wang, H.-B., Dembo, M., Hanks, S.K., Wang, Y.L., Focal Adhesion Kinase Is Involved in Mechanosensing During Fibroblast Migration, *Proceedings of the National Academy of Sciences of the United States of America*, Vol. 98, No. 20 (2001), pp. 11295-11300.
- (22) Davies, P.F., Zilberberg, J., Helmke, B.P., Spatial Microstimuli in Endothelial Mechanosignaling, *Circulation Research*, Vol. 92 (2003), pp. 359-370.
- (23) Jean, R.P., Chen, C.S., Spector, A.A., Finite-Element Analysis of the Adhesion-Cytoskeleton-Nucleus Mechanotransduction Pathway During Endothelial Cell Rounding: Axisymmetric Model, *Trans ASME Journal of Biomechanical Engineering*, Vol. 127 (2005), pp. 594-600.
- (24) Dewey, C.F., Jr., Bussolari, S.R., Gimbrone, M.A. Jr., Davies, P.F., The Dynamic Response of Vascular Endothelial Cells to Fluid Shear Stress, *Trans ASME Journal of Biomechanical Engineering*, Vol. 103, (1981), pp. 177-184.
- (25) Warabi, E., Wada, Y., Kajiwara, H., Kobayashi, M., Koshiba, N., Hisada, T., Shibata, M., Ando, J., Tsuchiya, M., Kodama, T., Noguchi, N., Effect on Endothelial Cell Gene Expression of Shear Stress, Oxygen Concentration, and Low-Density Lipoprotein as Studied by A Novel Flow Cell Culture System, *Free Radical Biology & Medicine*, Vol. 37, (2004), pp. 682-694.
- (26) Galbraith, C.G., Skalak, R., Chien, S., Shear Stress Induces Spatial Reorganization of the Endothelial Cell Cytoskeleton, *Cell Motility and the Cytoskeleton*, Vol. 40 (1998), pp. 317-330.
- (27) Ingber, D.E., Tensegrity: the Architectural Basis of Cellular Mechanotransduction, *Annual Review of Physiology*, Vol. 59, (1997), pp. 575-599.

## Skin advanced glycation end product accumulation and muscle strength among adult men

Haruki Momma · Kaijun Niu · Yoritoshi Kobayashi · Lei Guan · Mika Sato · Hui Guo · Masahiko Chujo · Atsushi Otomo · Cui Yufei · Hiroko Tadaura · Tatsunori Saito · Takefumi Mori · Toshio Miyata · Ryoichi Nagatomi

Accepted: 7 December 2010

© The Author(s) 2010. This article is published with open access at Springerlink.com

**Abstract** Aging is associated with decreased skeletal muscle function. Increased levels of advanced glycation end products (AGEs) in skeletal muscle tissue are observed with advancing age and in diabetes. Although serum AGE level is negatively associated with grip strength in elderly people, it is unknown whether this association is present in adult males. To determine the relationship between AGE accumulation in tissue and muscle strength and power among Japanese adult men. Skin autofluorescence (AF) (a noninvasive method for measuring tissue AGEs), grip strength ( $n = 232$ ), and leg extension power ( $n = 138$ ) were measured in Japanese adult men [median (interquartile range) age, 46.0 (37.0, 56.0) years]. After adjustment for potential confounders, the adjusted means [95% confidence interval (CI)] for grip strength across the tertiles of skin AF were 44.5 (43.2, 45.9) kg for the lowest tertile, 42.0 (40.6, 43.3) kg for the middle tertile, and 41.7 (40.3, 43.1) kg for the highest tertile ( $P$  for trend  $< 0.01$ ). Moreover, the adjusted geometric means (95% CI) of leg

extension power across the tertiles of skin AF were 17.8 (16.6, 19.1) W/kg for the lowest tertile, 17.5 (16.4, 18.7) W/kg for the middle tertile, and 16.0 (14.9, 17.1) W/kg for the highest tertile ( $P$  for trend = 0.04). Among Japanese adult men, participants with higher skin AF had lower muscle strength and power, indicating a relationship between AGE accumulation and muscle strength and power. A long-term prospective study is required to clarify the causality.

**Keywords** Advanced glycation end products · Leg extension power · Grip strength · Carbonyl stress · Oxidative stress

### Introduction

Ageing involves systemic accumulation of advanced glycation end products (AGEs), a diverse class of compounds resulting from glycation process under the strong influence of oxidative or carbonyl stress (Schleicher et al. 1997). In diabetic patients, increased accumulation of AGEs is observed (Schleicher et al. 1997; Singh et al. 2001). A common consequence of AGE accumulation is covalent cross-linking of AGEs to proteins, which leads to increased stiffness of protein matrix, impeding function and increasing resistance to removal of cross-linked proteins by proteolysis in various tissues and organs leading to impaired organ functions (Singh et al. 2001). Diabetic patients with end-stage renal disease had twice the concentrations of AGE in tissues compared with diabetic patients without renal disease (Makita et al. 1991).

Accumulation of AGE in the skeletal muscle tissue in elderly persons is suggested as one of the causes of decreased muscle force production (Haus et al. 2007).

Communicated by Arnold de Haan.

H. Momma · Y. Kobayashi · L. Guan · M. Sato · H. Guo · M. Chujo · A. Otomo · C. Yufei · H. Tadaura  
Department of Medicine and Science in Sports and Exercise,  
Tohoku University Graduate School of Medicine, Sendai, Japan

K. Niu · T. Saito · R. Nagatomi (✉)  
Division of Biomedical Engineering for Health and Welfare,  
Tohoku University Graduate School of Biomedical Engineering,  
2-1 Seiryō-machi, Aoba-ku, Sendai 980-8575, Japan  
e-mail: nagatomi@m.tains.tohoku.ac.jp

T. Mori · T. Miyata  
United Centers for Advanced Research and Translational  
Medicine, Tohoku University Graduate School of Medicine,  
Sendai, Japan

Published online: 25 December 2010

 Springer



Diabetic status accelerates AGE accumulation in skeletal muscle tissue in rats (Snow et al. 2006; Snow and Thompson 2009). In cross sectional studies, the levels of blood *N*<sup>c</sup>-carboxymethyl-lysine (CML), a major AGE in vivo, were negatively associated with muscle function in groups of elderly population (Dalal et al. 2009; Semba et al. 2010). Since AGE gradually accumulates along the course of aging even without diabetes, it is possible that the level of AGE accumulation may be inversely associated with muscle strength and power.

Using a simple autofluorescent measurement of AGE levels in the skin, we examined the association between AGE accumulation and muscle strength and power in a population of Japanese adult men.

## Methods

### Study participants

The study participants consisted of adult men, who had been enrolled in a prospective study of the risk factors for lifestyle-related illnesses or health status among adult employees in Japan. Participants received annual health examination including anthropometric measurements, hematological examinations and additional assessment including muscle strength and power measurement in year 2009. The details of this study have been described elsewhere (Guo et al. 2010).

The sample selection process is described in Fig. 1. In 2009, 1,263 participants were enrolled in the annual examinations for lifestyle-related illnesses and health status. Of those enrolled, 1,215 participants agreed to join the survey, providing their informed consent for data analysis (response rate, 96.2%). Because the number of female subjects was relatively small ( $n = 282$ ), females were excluded from the analyses. Those who underwent skin AF measurement were randomly selected ( $n = 518$ ). 272 participants who had lower skin reflection (<10%) were also excluded (details described in the skin autofluorescence section below). As a result of these exclusions, the numbers of subjects included in the analyses for the relationship between skin AF and grip strength (analysis I) and leg extension power (analysis II) were 232 and 138, respectively. The protocol of this study was approved by the Institutional Review Board of the Tohoku University Graduate School of Medicine.

### Skin autofluorescence (AF)

Skin AGE accumulation was assessed based on skin AF using an autofluorescence reader (AGE Reader; Diagnostics, Groningen, The Netherlands) as described previously

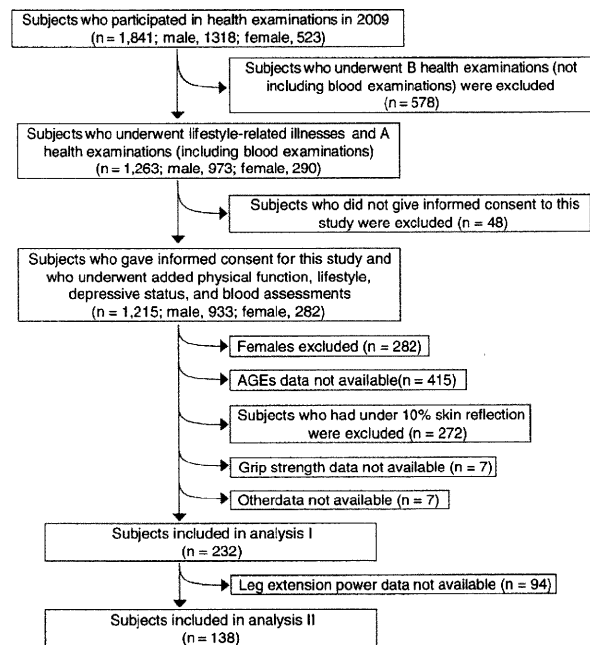


Fig. 1 Flow chart of the sample selection process

(Meerwaldt et al. 2004). The AGE Reader consists of a tabletop box equipped with an excitation light source. Each measurement took approximately 30 s to complete by an independent observer. Excitation light in the wavelength range of 300–420 nm is projected onto the skin surface through a 1-cm<sup>2</sup> hole. The intensity of light emitted from the skin at wavelengths between 420 and 600 nm is measured with a spectrometer via a glass fiber. Skin AF is calculated by dividing the mean value of the emitted light intensity per nm between 420 and 600 nm by the mean value of the excitation light intensity per nm between 300 and 420 nm; the result is expressed in arbitrary units (AU) and multiplied by 100 for easier evaluation. Skin AF has been validated to correspond to specific AGEs measured in human skin biopsy samples in several patient groups and healthy controls (Meerwaldt et al. 2004, 2005). The intra-assay coefficient of variation for repeated AF reader measurement on the same day was 5.0% (Meerwaldt et al. 2004).

All autofluorescence measurements were performed at room temperature on the volar side of the lower right arm, approximately 10–15 cm below the elbow fold, with the participants in a seated position. Care was taken to perform the measurement at a normal skin site, without visible vessels, scars, lichenification, or other skin abnormalities. The arm of each subject was covered with a black cloth in order to avoid any influence of external light during the measurement. Since skin pigmentation influences autofluorescence measurement, in particular when skin reflection is below 10%, autofluorescence values were not used

in this study when skin reflection was below 10% (Na et al. 2001).

### Muscle strength and power

Grip strength and leg extension power were measured. Grip strength was measured with a digital Smedley-type hand dynamometer (T.K.K.5401; Takei Scientific Instruments Co., Ltd, Niigata, Japan). The participants were told to adjust the device for hand comfort and fit and to place their arm in a relaxed, stationary position. Highest grip strength force of either right or left arm was used as representative grip strength.

Leg extension power was measured by Aneropress 3500 (Combi Wellness, Tokyo, Japan). Each participant was placed well back on a seat, the waist was fixed with a belt, and the knee joint angled at 90°. Isometric contractions lasted for 5 s each and were separated by 15-s rest intervals. Peak power was detected, calculated, and recorded in watts with a microcomputer. The highest measurement among five trials was recorded as “isometric strength performance.” To reduce the bias related to differences in body mass, leg extension power was expressed as the peak of the leg power relative to body weight (W/kg).

### Assessment of other variables

Depressive symptoms were assessed according to the Japanese version (Fukuda and Kobayashi 1973) of the Self-Rating Depression Scale (SDS). Participants were considered as depressive when SDS score was 45 or more (Fountoulakis et al. 2001). Blood pressure (BP) in the left upper arm was measured twice using an automatic device (YAMASU605P; Kenzmedico Co. Ltd., Saitama, Japan) following a 5-min rest in the sitting position. The mean values were used as the BP value.

Blood samples were drawn from the antecubital vein, with minimal tourniquet use, while the subjects were seated. Specimens were collected in siliconized vacuum glass tubes containing sodium fluoride for fasting blood glucose and no additives for lipid analyses. Fasting blood glucose concentration was measured by enzymatic methods (Eerotec, Tokyo, Japan). The triglyceride (TG), low-density lipoprotein cholesterol (LDL-C), and high-density lipoprotein cholesterol (HDL-C) concentrations were measured by enzymatic methods using appropriate kits (Sekisui Medical, Tokyo, Japan).

Information on age, smoking status (never, former, or currently smoking), alcohol-drinking status (never,  $\geq 1$  day/week, or 7 days/week), occupation (desk work or non-desk work), history of physical illness and current medication use (“yes” or “no”) of the participants were obtained from a questionnaire. The educational level was

assessed by determining the last grade level and divided into two categories: less than college level or college-level and above. Levels of daily physical activity (PA) were estimated using the International Physical Activity Questionnaire (Japanese version) (Craig et al. 2003). PA was categorized into tertiles with similar numbers of individuals in each group (low, middle, or high). Total energy consumption and vitamin C intake were estimated using a brief self-administered diet history questionnaire (Sasaki 2005). A diagnosis of metabolic syndrome (MS) was defined according to the modified Japanese criteria [defined by the Japanese Society for the Study of Obesity (JASSO)] (Matsuzawa 2005).

### Statistical analysis

All statistical analyses were performed using the SPSS 17.0 statistical software package for Windows (SPSS, Inc., Chicago, IL, USA).

In this study, because the distribution of all continuous variables, except for grip strength and systolic blood pressure, was not normal, the common logarithm was applied to normalize the data before statistical analysis. The Spearman rank correlation test was performed. ANCOVA was used to examine the relationships between skin AF and grip strength (analysis I,  $n = 232$ ) or log-transformed leg extension power (analysis II,  $n = 138$ ), adjusting for age and body mass index (model 1); all of the above parameters, in addition to PA, smoking status, drinking status, depressive symptoms, educational level, occupation, and total energy consumption, were used in model 2; all parameters in model 2 plus MS, diabetes, and kidney disease were used in model 3; and all parameters in model 3 plus vitamin C intake were used in model 4 (Fig. 1). ANCOVA was performed with the forced entry of all factors considered to be potential covariates. Bonferroni-corrected  $P$  values were used for comparisons between groups differing in skin AF. All  $P$  values for linear trends were calculated; all tests for statistical significance were two sided, and  $P < 0.05$  was defined as statistically significant.

### Results

The number of participants with skin reflection above 10% was 246 (47.5%), and the median (interquartile range) skin AF was 1.98 (1.78, 2.18) AU. The participant characteristics according to the tertiles of skin AF in analysis I are presented in Table 1. Subjects in the highest tertile of skin AF tended to be older and had a higher fasting glucose concentration ( $P$  for trend  $< 0.01$  and  $0.06$ , respectively); this group also had a higher percentage of current smokers compared with that in the lowest tertile ( $P$  for trend  $< 0.01$ ). Otherwise, no

**Table 1** Characteristics of the participants according to the tertiles of skin autofluorescence in analysis I ( $n = 232$ )

Range (unit, AU)	Tertiles of skin autofluorescence			<i>P</i> for trend <sup>a</sup>
	Low ( $n = 78$ ) (1.28–1.84)	Middle ( $n = 77$ ) (1.84–2.09)	High ( $n = 77$ ) (2.09–4.44)	
Age (years)	40.0 (35.0, 51.0)	45.0 (38.0, 57.0)	52.0 (40.0, 58.5)	<0.01
BMI (kg/m)	23.7 (22.1, 25.7)	23.7 (21.8, 25.9)	23.6 (21.7, 26.2)	0.89
Waist circumference (cm)	84.0 (77.8, 91.0)	86.0 (79.5, 90.5)	85.0 (80.0, 91.5)	0.29
SBP (mmHg)	130.0 (120.0, 137.3)	129.0 (116.0, 139.0)	130.0 (120.0, 142.0)	0.42
DBP (mmHg)	80.0 (74.0, 90.0)	80.0 (76.0, 88.5)	84.0 (74.0, 90.0)	0.44
Fasting blood glucose (mg/dl)	92.0 (88.8, 97.5)	93.0 (88.0, 100.0)	95.0 (88.5, 103.5)	0.06
TG (mg/dl)	110.5 (69.5, 153.5)	141.0 (79.5, 198.5)	131.0 (86.0, 186.5)	0.09
LDL (mg/dl)	120.0 (93.0, 139.0)	121.0 (95.0, 133.0)	122.0 (109.0, 144.5)	0.21
HDL (mg/dl)	53.0 (45.5, 63.3)	50.0 (42.5, 59.0)	52.0 (42.5, 56.5)	0.15
Total energy intake (kcal/d)	1910.9 (1599.7, 2409.1)	1806.8 (1569.9, 2201.5)	1747.7 (1416.0, 2267.8)	0.39
Vitamin C intake ([mg/d]/2000 kcal)	84.0 (61.4, 121.9)	93.8 (73.1, 128.6)	95.9 (66.7, 126.4)	0.72
High PA (%; median values: 48.0 METs-h/week)	43.6	28.6	40.3	0.09
Middle PA (%; median values: 12.1 METs-h/week)	39.7	46.8	36.4	0.05
Smoking status				
Current (%)	29.5	40.3	49.4	0.04
Former (%)	12.8	20.8	10.4	0.17
Drinking status				
7 drinks/week (%)	28.2	29.9	23.4	0.64
≥1 drinks/week (%)	59.0	54.5	58.4	0.83
Depressive symptoms (SDS ≥ 45, %)	30.8	31.2	29.9	0.98
Education (≥college, %)	43.6	35.1	40.3	0.55
Desk work (%)	87.2	74.0	77.9	0.12
Diabetes (%)	6.4	10.4	9.1	0.67
Kidney disease (%)	2.6	1.3	6.5	0.23
MS (JASSO, %)	20.5	24.7	27.3	0.61

Data are medians (interquartile range) or proportions

AU arbitrary units, BMI body mass index, SBP systolic blood pressure, DBP diastolic blood pressure, TG triglyceride, LDL low-density lipoprotein cholesterol, HDL high-density lipoprotein-cholesterol, PA physical activity, SDS self-rating depression scale, MS metabolic syndrome, JASSO Japanese Society for the Study of Obesity

<sup>a</sup> Analysis of variance or logistic regression

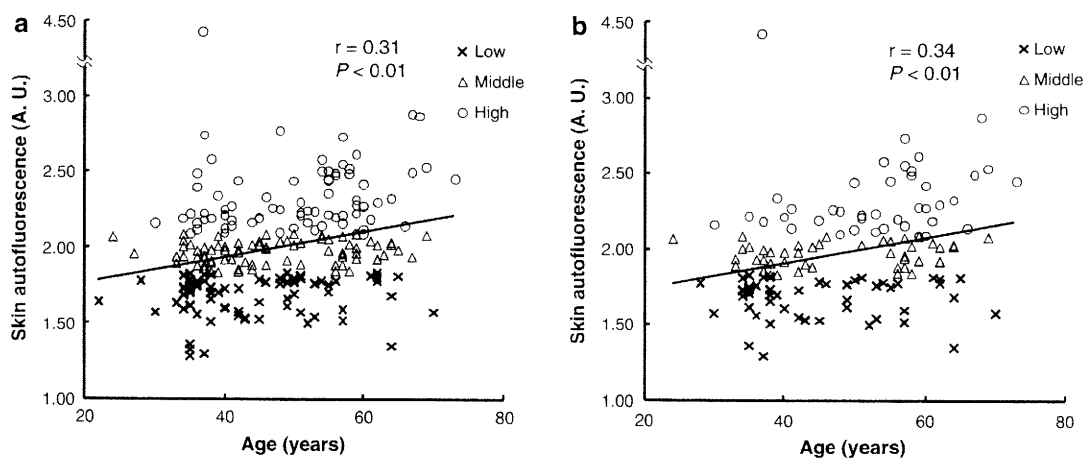
significant differences were observed among the tertiles of skin AF. In Fig. 2a, outlier (skin AF = 4.44 A.U.) was a person with both diabetes and kidney disease, and skin AF correlated with age ( $r = 0.31$ ,  $P < 0.01$ ).

Table 2 shows the relationship of skin AF tertiles to grip strength. In the final multivariate models, the adjusted means [95% confidence interval (CI)] of the grip strength across the tertiles of skin AF was 44.5 (43.2, 45.9) kg for the lowest tertile, 42.0 (40.6, 43.3) kg for the middle tertile, and 41.7 (40.3, 43.1) kg for the highest tertile ( $P$  for trend < 0.01). The adjusted mean grip strength was 6.3% lower for the highest tertile of skin AF than for the lowest tertile of skin AF (Bonferroni-corrected  $P$  value = 0.01).

To assess the relationship between skin AF tertiles and leg extension power, we performed an additional analysis (analysis II) that excluded those subjects who did not

undergo the leg extension power test ( $n = 138$ ). Table 3 shows the participant characteristics according to tertiles of skin AF in analysis II. In analysis II, subjects in the highest tertile of skin AF were older and had higher fasting glucose concentrations compared with those in the lowest tertile ( $P$  for trend < 0.01 and 0.02, respectively). Although no significant difference was observed in the percentage of current smokers, the prevalence of diabetes in the highest tertile of skin AF tended to be higher than that of the lowest tertile ( $P$  for trend = 0.05). In the Spearman rank correlation test, skin AF correlated with age ( $r = 0.34$ ,  $P < 0.01$ ) (Fig. 2b).

Table 4 shows the relationship of the tertiles of skin AF with leg extension power. In the final multivariate models, the adjusted geometric mean (95% CI) of log-transformed leg extension power across the tertiles of skin AF was 17.8



**Fig. 2** Correlation between skin autofluorescence and age in analysis I (a) and analysis II (b). Spearman rank correlation test was performed. Cross, triangle, and circle symbols are represented as the lower, middle, and higher tertile of skin autofluorescence, respectively

**Table 2** Relationship of the tertile of skin autofluorescence with grip strength ( $n = 232$ )

Range (unit, AU)	Tertiles of skin autofluorescence			<i>P</i> for trend <sup>a</sup>
	Low (1.28–1.84)	Middle (1.84–2.09)	High (2.09–4.44)	
No. of participants	78	77	77	–
Grip strength (kg)				
Crude	44.7 (43.3, 46.1)	41.7 (40.3, 43.1) <sup>f</sup>	41.8 (40.4, 43.2) <sup>f</sup>	<0.01
Model 1 <sup>b</sup>	44.3 (43.0, 45.7)	41.8 (40.4, 43.1) <sup>f</sup>	42.1 (40.8, 43.5)	0.03
Model 2 <sup>c</sup>	44.5 (43.2, 45.9)	42.0 (40.7, 43.4) <sup>f</sup>	41.6 (40.2, 43.0) <sup>f</sup>	<0.01
Model 3 <sup>d</sup>	44.5 (43.2, 45.9)	42.0 (40.7, 43.3) <sup>f</sup>	41.7 (40.3, 43.0) <sup>f</sup>	<0.01
Model 4 <sup>e</sup>	44.5 (43.2, 45.9)	42.0 (40.6, 43.3) <sup>f</sup>	41.7 (40.3, 43.1) <sup>f</sup>	<0.01

Data are means (95% confidence interval). Unit of grip strength is kg

AU arbitrary units

<sup>a</sup> Analysis of variance or analysis of covariance

<sup>b</sup> Adjusted for age (continuous variables, log-transformed), body mass index (continuous variables, log-transformed)

<sup>c</sup> Additionally adjusted for physical activity (tertiles), smoking status (never, former, or current), drinking status (never,  $\geq 1$  drinks/week, or 7 drinks/week), depressive symptoms (self-rating depression scale  $\geq 45$ ), educational level ( $\geq$ college), occupation (desk work or non-desk work), and total energy consumption (continuous variables, log-transformed)

<sup>d</sup> Additionally adjusted for metabolic syndrome (Japanese Society for the Study of Obesity) (no or yes), diabetes (no or yes), and kidney disease (no or yes)

<sup>e</sup> Additionally adjusted for dietary intake of vitamin C (continuous variables, log-transformed)

<sup>f</sup> Significantly different from lowest skin autofluorescence tertile (Bonferroni correction),  $P < 0.05$

(16.6, 19.1) W/kg for the lowest tertile, 17.5 (16.4, 18.7) W/kg for the middle tertile, and 16.0 (14.9, 17.1) W/kg for the highest tertile ( $P$  for trend = 0.04).

### Discussion

The present study examined the relationship between skin AF representing AGE accumulation and muscle strength and power among Japanese adult men. Consistent

with previous studies (Dalal et al. 2009; Semba et al. 2010), our results showed that the level of skin AF was independently associated with muscle strength and power. These results suggest that greater AGE accumulation is associated with reduced muscle strength and power not only in older people but also in younger adults, and that AGE accumulation may be a predisposing factor for muscle force reduction along the course of aging finally leading to sarcopenia.

There is an increasing evidence supporting the hypothesis that AGEs may play a role in the decline of muscle



**Table 3** Characteristics of the participants according to the tertiles of skin autofluorescence in analysis II ( $n = 138$ )

Range (unit, AU)	Tertiles of skin autofluorescence			P for trend <sup>a</sup>
	Low ( $n = 46$ ) (1.28–1.84)	Middle ( $n = 46$ ) (1.84–2.09)	High ( $n = 46$ ) (2.09–4.44)	
Age (years)	42.5 (35.0, 53.3)	43.5 (37.0, 57.0)	55.5 (46.8, 60.0)	<0.01
BMI (kg/m)	23.7 (21.7, 25.6)	23.8 (21.9, 25.8)	23.4 (21.5, 25.9)	0.92
Waist circumference (cm)	84.0 (77.0, 92.0)	87.0 (78.8, 92.0)	86.0 (80.8, 91.3)	0.38
SBP (mmHg)	128.0 (119.5, 137.8)	130.0 (115.5, 140.3)	132.0 (117.5, 140.0)	0.59
DBP (mmHg)	80.0 (73.5, 88.3)	80.0 (73.5, 90.3)	81.5 (75.5, 86.3)	0.61
Fasting blood glucose (mg/dl)	93.0 (88.8, 100.3)	90.5 (88.0, 96.0)	96.0 (88.5, 105.3)	0.02
TG (mg/dl)	111.5 (69.5, 154.3)	140.0 (75.8, 187.8)	131.5 (84.0, 186.0)	0.41
LDL (mg/dl)	117.5 (91.0, 137.5)	123.0 (105.3, 133.0)	121.0 (109.0, 152.8)	0.27
HDL (mg/dl)	53.0 (45.5, 61.8)	52.0 (43.8, 59.0)	53.5 (44.0, 60.0)	0.73
Total energy intake (kcal/d)	1887.1 (1509.9, 2378.0)	1783.3 (1580.2, 2244.2)	1655.2 (1354.0, 2314.1)	0.47
Vitamin C intake (mg/dl)/2000 kcal)	82.4 (61.4, 127.7)	97.1 (65.9, 124.5)	103.7 (76.2, 132.5)	0.36
High PA (% , median values: 48.0 METs·h/week)	39.1	28.3	32.6	0.54
Middle PA (% , median values: 12.1 METs·h/week)	32.6	34.8	32.6	0.97
Smoking status				
Current (%)	28.3	34.8	41.3	0.43
Former (%)	10.9	19.6	15.2	0.52
Drinking status				
7 drinks/week (%)	28.3	34.8	17.4	0.17
≥1 drinks/week (%)	60.9	52.2	56.5	0.73
Depressive symptoms (SDS ≥ 45, %)	28.3	34.8	32.6	0.56
Education (≥college, %)	39.1	37.0	39.1	0.97
Desk work (%)	89.1	69.6	84.8	0.05
Diabetes (%)	6.5	6.5	19.6	0.09
Kidney disease (%)	2.2	2.2	2.2	1.00
MS (JASSO, %)	19.6	26.1	21.7	0.75

Data are medians (interquartile range) or proportions

AU arbitrary units, BMI body mass index, SBP systolic blood pressure, DBP diastolic blood pressure, TG triglyceride, LDL low-density lipoprotein cholesterol, HDL high-density lipoprotein-cholesterol, PA physical activity, SDS self-rating depression scale, MS metabolic syndrome, JASSO Japanese Society for the Study of Obesity

<sup>a</sup> Analysis of variance or logistic regression

function, which may eventually lead to sarcopenia in the older age. First, AGE accumulation in skeletal muscle is greater in fast muscle fiber types, which are well known to possess a faster shortening velocity and larger force production (Snow and Thompson 2009). Second, AGE-modified proteins in skeletal muscle include several critical enzymes involved in energy production, such as creatine kinase (Snow et al. 2007). Third, glycation of skeletal muscle myosin changed the structural property of the protein and reduced simultaneously the in vitro motility speed (Ramamurthy et al. 2001). Moreover, because the binding of AGEs to RAGE results in depletion of cellular antioxidant defense mechanisms and the generation of oxygen-free radicals (Schmidt et al. 1994), oxidant damage to myofibrillar proteins may play a role in the age-related reduction of contractile capacity (Thompson 2009). AGE–RAGE

interaction also induces microcirculatory dysfunction by endothelial dysfunction or inflammation (Brownlee 2001; Payne 2006). Thus, AGE accumulation may contribute to decreased muscle function with aging through a variety of mechanisms.

It is well known that vitamin C is one of the primary antioxidants. Because greater intake of vitamin C was independently associated with muscle strength (Cesari et al. 2004), dietary intake of vitamin C may potentially influence the relationship between skin AF and muscle strength and power. In this study, because the relationship between higher skin AF and lower muscle strength and power remained even after adjusting the intake of vitamin C, higher skin AF could be associated with lower muscle strength and power independent of dietary intake of vitamin C in healthy adult men.

**Table 4** Relationship of the tertile of skin autofluorescence with log-transformed leg extension power ( $n = 138$ )

Range (unit, AU)	Tertiles of skin autofluorescence			<i>P</i> for trend <sup>a</sup>
	Low (1.29–1.81)	Middle (1.81–2.07)	High (2.07–4.44)	
No. of participants	46	46	46	–
Leg extension power (W/kg)				
Crude	18.6 (17.0, 20.0)	17.4 (16.2, 19.1)	15.5 (14.5, 16.2) <sup>f</sup>	<0.01
Model 1 <sup>b</sup>	18.2 (17.0, 19.5)	17.4 (16.2, 18.6)	15.8 (14.8, 17.0) <sup>f</sup>	0.01
Model 2 <sup>c</sup>	17.8 (16.6, 19.1)	17.4 (16.2, 18.6)	15.8 (14.8, 17.4)	<0.05
Model 3 <sup>d</sup>	17.8 (16.6, 19.1)	17.4 (16.2, 18.6)	16.2 (14.8, 17.4)	0.05
Model 4 <sup>e</sup>	17.8 (16.6, 19.1)	17.5 (16.4, 18.7)	16.0 (14.9, 17.1)	0.04

Data are geometric means (95% confidence interval). Unit of leg extension power is W/kg

AU arbitrary units

<sup>a</sup> Analysis of variance or analysis of covariance

<sup>b</sup> Adjusted for age (continuous variables, log-transformed), body mass index (continuous variables, log-transformed)

<sup>c</sup> Additionally adjusted for physical activity (tertiles), smoking status (never, former, or current), drinking status (never,  $\geq 1$  drinks/week, or  $\geq 7$  drinks/week), depressive symptoms (self-rating depression scale  $\geq 45$ ), educational level ( $\geq$ college), occupation (desk work, or non-desk work), and total energy consumption (continuous variables, log-transformed)

<sup>d</sup> Additionally adjusted for metabolic syndrome (Japanese Society for the Study of Obesity) (no or yes), diabetes (no or yes), and kidney disease (no or yes)

<sup>e</sup> Additionally adjusted for dietary intake of vitamin C (continuous variables, log-transformed)

<sup>f</sup> Significantly different from lowest skin autofluorescence tertile (Bonferroni correction),  $P < 0.05$

In this study, skin AF was used as a measure for skin AGE accumulation. Previous studies reported that skin AF is correlated with blood AGEs (Tanaka et al. 2009), or not (Hartog et al. 2008). In this study, our findings conform to previous studies which measured circulating CML (Dalal et al. 2009; Semba et al. 2010). Thus, it is speculated that skin AF is potentially correlated with blood AGEs in our participants.

This study has other limitations. First, this study focused only on men. Whether the relationship is present in younger women is unknown. Moreover, although we adjusted for confounders such as lifestyle factors or disease, we cannot exclude the possibility that muscle strength and power was affected by other factors associated with lifestyle, disease, or protein damage in skeletal tissue that correlate with AGE accumulation. Finally, because this study was a cross-sectional study, we could not conclude whether AGE accumulation in tissue decreased muscle strength and power. A prospective study or trial should be undertaken to further confirm the causal relationship between AGE accumulation and muscle strength and power.

## Conclusion

The participants—apparently healthy adult men—with higher skin AF associated with AGE accumulation had lower muscle strength and power. Further studies are needed to confirm whether increased AGE accumulation in

tissue predict a decline in muscle strength and power with advancing age in younger adults.

**Acknowledgments** We gratefully acknowledge all the subjects for participating in our study and the Sendai Oroshisho Center for allowing us to perform the study. This work was supported by a Grant-in-Aid under the “Knowledge Cluster Initiative” from the Ministry of Education, Culture, Sports, Science and Technology of Japan. The present study complies with the current laws of Japan and the protocol of the present study was approved by the Institutional Review Board of the Tohoku University Graduate School of Medicine.

**Conflict of interest** None of the authors have any conflicts of interest to disclose.

**Open Access** This article is distributed under the terms of the Creative Commons Attribution Noncommercial License which permits any noncommercial use, distribution, and reproduction in any medium, provided the original author(s) and source are credited.

## References

- Brownlee M (2001) Biochemistry and molecular cell biology of diabetic complications. *Nature* 414:813–820
- Cesari M, Pahor M, Bartali B, Cherubini A, Penninx BW, Williams GR, Atkinson H, Martin A, Guralnik JM, Ferrucci L (2004) Antioxidants and physical performance in elderly persons: the Invecchiare in Chianti (InCHIANTI) study. *Am J Clin Nutr* 79:289–294
- Craig CL, Marshall AL, Sjostrom M, Bauman AE, Booth ML, Ainsworth BE, Pratt M, Ekelund U, Yngve A, Sallis JF, Oja P (2003) International physical activity questionnaire: 12-country reliability and validity. *Med Sci Sports Exerc* 35:1381–1395

- Dalal M, Ferrucci L, Sun K, Beck J, Fried LP, Semba RD (2009) Elevated serum advanced glycation end products and poor grip strength in older community-dwelling women. *J Gerontol A Biol Sci Med Sci* 64:132–137
- Fountoulakis KN, Iacovides A, Samolis S, Kleanthous S, Kaprinis SG, St. Kaprinis G, Bech P (2001) Reliability, validity and psychometric properties of the Greek translation of the Zung Depression Rating Scale. *BMC Psychiatry* 1:6
- Fukuda K, Kobayashi S (1973) A study on a self-rating depression scale (author's transl). *Seishin Shinkeigaku Zasshi* 75:673–679 (in Japanese)
- Guo H, Niu K, Monma H, Kobayashi Y, Guan L, Sato M, Minamishima D, Nagatomi R (2010) Association of Japanese dietary pattern with serum adiponectin concentration in Japanese adult men. *Nutr Metab Cardiovasc Dis*. doi:10.1016/j.numecd.2010.06.006
- Hartog JW, Hummel YM, Voors AA, Schalkwijk CG, Miyata T, Huisman RM, Smit AJ, Van Veldhuisen DJ (2008) Skin-autofluorescence, a measure of tissue advanced glycation end-products (AGEs), is related to diastolic function in dialysis patients. *J Card Fail* 14:596–602
- Haus JM, Carrithers JA, Trappe SW, Trappe TA (2007) Collagen, cross-linking, and advanced glycation end products in aging human skeletal muscle. *J Appl Physiol* 103:2068–2076
- Makita Z, Radoff S, Rayfield EJ, Yang Z, Skolnik E, Delaney V, Friedman EA, Cerami A, Vlassara H (1991) Advanced glycosylation end products in patients with diabetic nephropathy. *N Engl J Med* 325:836–842
- Matsuzawa Y (2005) Metabolic syndrome—definition and diagnostic criteria in Japan. *J Atheroscler Thromb* 12:301
- Meerwaldt R, Graaff R, Oomen PH, Links TP, Jager JJ, Alderson NL, Thorpe SR, Baynes JW, Gans RO, Smit AJ (2004) Simple non-invasive assessment of advanced glycation endproduct accumulation. *Diabetologia* 47:1324–1330
- Meerwaldt R, Hartog JW, Graaff R, Huisman RJ, Links TP, den Hollander NC, Thorpe SR, Baynes JW, Navis G, Gans RO, Smit AJ (2005) Skin autofluorescence, a measure of cumulative metabolic stress and advanced glycation end products, predicts mortality in hemodialysis patients. *J Am Soc Nephrol* 16:3687–3693
- Na R, Stender IM, Henriksen M, Wulf HC (2001) Autofluorescence of human skin is age-related after correction for skin pigmentation and redness. *J Invest Dermatol* 116:536–540
- Payne GW (2006) Effect of inflammation on the aging microcirculation: impact on skeletal muscle blood flow control. *Microcirculation* 13:343–352
- Ramamurthy B, Hook P, Jones AD, Larsson L (2001) Changes in myosin structure and function in response to glycation. *FASEB J* 15:2415–2422
- Sasaki S (2005) Serum biomarker-based validation of a brief-type self-administered diet history questionnaire for Japanese subjects. The Study Group of Ministry of Health, Labor and Welfare of Japan, Tanaka H, chairman, “A research for assessment of nutrition and dietary habit in “Kenko Nippon 21”, 10–42 (in Japanese)
- Schleicher ED, Wagner E, Nerlich AG (1997) Increased accumulation of the glycoxidation product N(epsilon)-(carboxymethyl)lysine in human tissues in diabetes and aging. *J Clin Invest* 99:457–468
- Schmidt AM, Hori O, Brett J, Yan SD, Wautier JL, Stern D (1994) Cellular receptors for advanced glycation end products. Implications for induction of oxidant stress and cellular dysfunction in the pathogenesis of vascular lesions. *Arterioscler Thromb* 14:1521–1528
- Semba RD, Bandinelli S, Sun K, Guralnik JM, Ferrucci L (2010) Relationship of an advanced glycation end product, plasma carboxymethyl-lysine, with slow walking speed in older adults: the InCHIANTI study. *Eur J Appl Physiol* 108:191–195
- Singh R, Barden A, Mori T, Beilin L (2001) Advanced glycation end-products: a review. *Diabetologia* 44:129–146
- Snow LM, Thompson LV (2009) Influence of insulin and muscle fiber type in nepsilon-(carboxymethyl)-lysine accumulation in soleus muscle of rats with streptozotocin-induced diabetes mellitus. *Pathobiology* 76:227–234
- Snow LM, Lynner CB, Nielsen EM, Neu HS, Thompson LV (2006) Advanced glycation end product in diabetic rat skeletal muscle in vivo. *Pathobiology* 73:244–251
- Snow LM, Fugere NA, Thompson LV (2007) Advanced glycation end-product accumulation and associated protein modification in type II skeletal muscle with aging. *J Gerontol A Biol Sci Med Sci* 62:1204–1210
- Tanaka T, Katoh T, Asai J, Nemoto F, Suzuki H, Asahi K, Sato K, Sakaue M, Miyata T, Watanabe T (2009) Relationship of skin autofluorescence to cardiovascular disease in Japanese hemodialysis patients. *Ther Apher Dial* 14:334–340
- Thompson LV (2009) Age-related muscle dysfunction. *Exp Gerontol* 44:106–111

## Effect of office-based brief high-impact exercise on bone mineral density in healthy premenopausal women: the Sendai Bone Health Concept Study

Kaijun Niu · Riikka Ahola · Hui Guo · Raija Korpelainen · Jin Uchimarū · Aki Vainionpää · Kyoko Sato · Aiko Sakai · Sinikka Salo · Koshi Kishimoto · Eiji Itoi · Shoko Komatsu · Timo Jämsä · Ryoichi Nagatomi

Received: 30 September 2009 / Accepted: 28 January 2010  
© The Japanese Society for Bone and Mineral Research and Springer 2010

**Abstract** Although there is ample evidence supporting the effectiveness of physical activity in the prevention and treatment of osteoporosis, there are no previous studies to

Trial Registration: <http://www.umin.ac.jp/ctr/index.htm>  
Identifier: UMIN000000533.

K. Niu · H. Guo · R. Nagatomi (✉)  
Division of Biomedical Engineering for Health and Welfare,  
Tohoku University Graduate School of Biomedical Engineering,  
2-1 Seiryō-machi, Aoba-ku, Sendai 980-8575, Japan  
e-mail: nagatomi@mail.tains.tohoku.ac.jp

R. Ahola · R. Korpelainen · A. Vainionpää · S. Salo · T. Jämsä  
Department of Medical Technology, University of Oulu,  
Oulu, Finland

R. Korpelainen  
Department of Sports and Exercise Medicine,  
Deaconess Institute of Oulu, Oulu, Finland

R. Korpelainen  
Unit of General Practice, Institute of Health Sciences,  
University of Oulu, Oulu, Finland

J. Uchimarū · K. Sato · S. Komatsu  
Faculty of Sports Science, Sendai University, Sendai, Japan

A. Vainionpää  
Department of Physical Medicine and Rehabilitation,  
Seinäjäki Central Hospital, Seinäjoki, Finland

A. Sakai · S. Salo  
Sendai Finland Wellbeing Center, Sendai, Japan

K. Kishimoto · E. Itoi  
Department of Orthopaedic Surgery, Tohoku University  
Graduate School of Medicine, Sendai, Japan

T. Jämsä  
Department of Diagnostic Radiology,  
Oulu University Hospital, Oulu, Finland

examine the effect of office-based brief high-impact exercise (HIE) on bone mineral density (BMD) in healthy premenopausal women. This study evaluated the effects of office-based HIE on BMD in healthy premenopausal Japanese women. Ninety-one healthy premenopausal women were randomized to receive stretching exercise (SE) or HIE (stretching, along with up to 5 × 10 vertical and versatile jumps) for 12 months. The BMD of the lumbar spine and proximal femur was measured using dual-energy X-ray absorptiometry. Several cardiovascular risk factors and leg strength also were assessed. An accelerometer-based recorder was used to measure daily impact loading in four 1-week samples. The progression of the HIE program was ensured by the accelerometer. Thirty-three women (71.7%) in the SE group and 34 (75.6%) in the HIE group completed the study. There was a significant difference in the change in the femoral neck BMD between the groups in favor of the HIE group [0.6% (95% CI: -0.4, 1.7) vs. -1.0% (95% CI: -2.2, 0.2)]. Adiponectin, LDL, HDL, and the leg strength of participants in both the groups improved during the intervention. These findings suggested that office-based brief HIE can be recommended for premenopausal women for preventing bone mineral loss.

**Keywords** Osteoporosis · Impact exercise · Bone mineral density · Accelerometer

### Introduction

Osteoporosis is a major risk factor for fractures in the elderly [1]. It has been estimated that there are more than 10 million osteoporotic patients in Japan, 70% of whom are female [2]. Incidence of fractures of the femoral neck, which severely impair the quality of life (QOL), has